

QUANTIFYING THERMAL EXPOSURES AND EFFECTS FOR CENTRAL VALLEY ANADROMOUS SALMONIDS

Draft Methods and Documentation

Authors: Alyssa FitzGerald, Sara John, Travis Apgar, and Benjamin Martin
University of California, Santa Cruz Agreement #16-048-150
15 July 2018

INTRODUCTION

The goal of this project is to develop a framework to quantify how temperature affects Central Valley salmonids and to describe studies needed to develop site-specific temperature criteria that are protective of Central Valley anadromous salmonids. A central part of this question is to determine whether Region 10 temperature criteria that were derived for salmonid populations in Oregon, Washington, Idaho, and Alaska (U.S. EPA 2003) are appropriate for salmonid populations in California. In other words, are California populations physiologically and behaviorally adapted to the thermal environments at the southernmost edge of their distribution?

Although there are several examples of salmonid populations physiologically adapting to their local thermal regime (e.g. Eliason et al. 2011, Poletto et al. 2017), a recent review found a paucity of data to compare the thermal tolerance of California vs. region 10 populations (Zillig et al. in prep). Due to the lack of data, Zillig et al. (in prep) conclude that Region 10 criteria should be used in California until sufficient comparative laboratory, field and modeling studies have been conducted to scientifically assess whether the temperature criteria should be adjusted for California anadromous salmonid populations.

Here we describe a set of modeling research tasks that – combined with the comparative laboratory and field studies recommended by Zillig et al. (in prep.) – will define thermal exposure and help set scientifically calculate the effects of temperature on different life stages of anadromous salmonid populations in the Central Valley. This work will be the first step to determine if Region 10 criteria are applicable to the Central Valley. When Region 10 thresholds cannot be met during particularly warm years, our framework will allow managers to compare thermal effects on different life stages in order to assess which life stages are the most vulnerable in space and time. Our work addresses three main research questions:

Q1. How can we quantify the thermal environment experienced by Central Valley salmonid populations, and how does it differ from Region 10 populations?

Q2. Can we improve site-specific temperature management in the Central Valley by using thermal performance curves?

Q3. What additional studies are needed in order to develop specific thermal thresholds for the different life stage of salmonids in the Central Valley?

To answer these questions, we need to know where (distribution) and when (phenology) different life stages of each population occurs, and what stream temperatures are associated with these life stages in space and time. Below, we describe our methodology behind the first two questions, provide examples using Chinook populations from the Central Valley, and discuss future analyses and implications. We end by providing recommendations of future studies required in order to establish site-specific thermal thresholds for salmonids in the Central Valley.

Q1. How can we quantify the thermal environment experienced by Central Valley salmonid populations, and how does it differ from Region 10 populations?

INTRODUCTION

In comparison with northerly populations, southern salmonids are exposed to warmer temperatures and more variable weather events, indicating that they may be 1) thermally adapted to the California climate, 2) phenotypically plastic, enabling them to tolerate warmer waters, or 3) at the extreme tolerance of thermal capacity, such that minor warming or extreme weather events could result in significant mortality and population loss. An important first step in addressing if California salmon are thermally adapted, phenotypically plastic, or at the extreme range of tolerance to their environment is to first determine if and how the thermal environment experienced by California populations differs from Region 10 populations. Comparisons of local studies tend to support the assumption that phenology and thermal exposure varies between ESUs, but a range-wide assessment of all ESUs for multiple life stages has not been undertaken. Comparison of populations in individual rivers (e.g. Sacramento River and Snake River) is overly simplistic and can miss broad spatial patterns, so here we analyze spatial and temporal patterns in temperature exposure for Central Valley populations in the context of all other populations in Region 10.

Calculating the thermal exposure of a population requires 1) knowledge of its distribution and phenology, and 2) the stream temperatures in space and time. Addressing Q1 is difficult for several reasons. First, because different life stages of salmon populations have different thermal sensitivities, and the thermal exposure of each life stage depends the life stage preceding it in time and space, a detailed understanding of both the distribution and phenology of each life stage is required. The second difficulty is that temperature in river networks is highly dynamic in time and space, but temperature data is sparse – a very small fraction of the hundreds of thousands of river km in the western U.S. have observed temperature data. We overcome these challenges by 1) aggregating presence points and distributions from multiple data sources to create the most complete distribution dataset possible for each life stage of each population, 2) developing a database of the phenology of each life stage of each population, and 3) applying a statistical stream network model that translates sparse temperature data into monthly stream temperature predictions for every river km in the western U.S.

The distribution and phenology databases allow us to examine spatial and temporal patterns for each ESU, run, and life stage. To test for potential differences in thermal exposure between groups, we will overlay our distribution and phenology datasets with stream temperature to examine spatial and temporal temperature patterns between different groupings, i.e. different life stages within and between populations. Specifically, we will determine if differences in thermal exposures are more extreme for particular life stages (e.g. adult migration vs. fry rearing) or runs (spring vs. fall). By comparing expected thermal exposures using a generic vs. population-specific phenology data we can quantify the degree to which phenology

buffers exposures to elevated temperatures for California populations. Finally, we quantify thermal exposure for California populations compared to those in Region 10, and determine which life-stages/runs/rivers within the Central Valley are exposed to temperatures near the Region 10 thresholds and may therefore be more vulnerable to incremental increases in temperature.

METHODS

Datasets

Distribution dataset

The distribution dataset defines spatial distributions of life stages for different populations. Occurrences were extracted August 2017-January 2018 from eight field-observational and distributional data sources¹. Linear distribution datasets (StreamNet and CalFish) were broken up into points separated by 1 km, then added to the observational dataset. Occurrences are accurate to 500 m, and each occurrence was defined by ESU, life stage, and month. To match the temporal limit of the stream temperature modeling project, occurrences prior to 1993 were removed. Missing information (e.g. if ESU or date was not listed) was filled in by spatially merging occurrences with ESUs (http://www.westcoast.fisheries.noaa.gov/maps_data/Species_Maps_Data.html) and by comparison to the phenology database (see below). The life stages defined were adults migrating, spawning, incubation, emergence, juvenile rearing, and juvenile outmigrating. We removed unspecified juveniles from the occurrence dataset unless the juvenile stage (i.e. rearing vs. outmigrating) was indicated. The current distribution dataset has over 200,000 verified occurrences. Occurrences for the Central Valley region may be found in Fig. 1.

Phenology database

We reviewed primary and secondary literature sources to develop a phenology database for each life history stage of each population (Appendix 1 Table S1.1, Appendix 1 List 1). If a recognized ESU contains multiple runs, we separated runs due to phenological differences and hereafter refer to all such groupings as populations. Often, phenological information was only available for an ESU on a monthly time-step, and our table reflects this. The peak month (or median if peak was unknown) of each life stage was defined. We plan to merge the table with ESU distributions in ArcGIS and make this dataset and its metadata (including sources) publically available.

¹ ASOD: obtained via California Dept. of Fish and Wildlife

CalFish: <http://www.calfish.org/DataandMaps/CalFishDataExplorer.aspx>

Global Biodiversity Information Facility: www.gbif.org

OBIS: www.iobis.org

StreamNet: <https://www.streamnet.org/>

U.S. EPA: <https://www.epa.gov/national-aquatic-resource-surveys/data-national-aquatic-resource-surveys>

U.S.G.S.: <https://aquatic.biodata.usgs.gov>

VertNet: <http://vertnet.org/>

Monthly stream temperature

Obtaining stream temperature involved expanding a pre-existing spatial stream network model (SSN) (Isaak et al. 2017), currently only available for August, to all months of the year in order to have a full picture of the habitat that is thermally available to salmonids at various life stages. SSNs have been shown to be an effective modeling strategy for stream temperature because they are able to account for the complex autocovariance structures inherent to stream temperature data (Peterson and Ver Hoef 2010, Rushworth et al. 2015, Isaak et al. 2017). Following Isaak et al. (2017), our SSN models includes three autocovariance functions: tail-down, tail-up, and Euclidean distance. Tail-down autocovariance functions are based on moving average functions in the downstream direction and allow correlation between sites that are flow-connected and sites that are flow-unconnected (Ver Hoef and Peterson 2010). Tail-up autocovariance functions are based on moving average functions in the upstream direction, allow correlation between sites that are connected by flow, and use spatial weighting to partition the moving average function at tributary confluences (Ver Hoef and Peterson 2010). An autocovariance function based on Euclidian distance (“as the bird flies”) is used to account for sources of autocorrelation not attributable to the network structure of rivers. Research has shown advantages in using a mixed model approach which combines multiple autocovariance functions (Peterson and Ver Hoef 2010).

We are expanding the results of Isaak et al. (2017) to multiple months of the year, and below is a summary of the SSN model. The model has the form:

$$y = X\beta + L\gamma + R\eta + z_{TU} + z_{TD} + z_{EUC} + \varepsilon$$

where y is a vector of observed water temperatures; X is a design matrix of covariate values; β is a vector of regression coefficients; L is a random-effects design matrix for location; γ is a vector of zero-mean, normally distributed random effects for location; R is a random-effects design matrix for year; η is a vector of zero-mean, normally distributed effects for year; z_{TU} , z_{TD} , and z_{EUC} are vectors of zero-mean random effects with an autocorrelation structure based on an exponential tail-up function with spatial weights determined by watershed area, an exponential tail-down function, and an exponential Euclidian function, respectively; and ε is a vector of independent and normally distributed random errors. The covariance matrix is given by:

$$\Sigma = \sigma^2_{\gamma}LL' + \sigma^2_{\eta}RR' + \sigma^2_{TU}C_{TU} + \sigma^2_{TD}C_{TD} + \sigma^2_{EUC}C_{EUC} + \sigma^2_{\varepsilon}I$$

where σ^2_{γ} , σ^2_{η} , σ^2_{TU} , σ^2_{TD} , σ^2_{EUC} , and σ^2_{ε} are variances for γ , η , z_{TU} , z_{TD} , z_{EUC} , and ε , respectively, and C_{TU} , C_{TD} , and C_{EUC} are autocorrelation matrices for z_{TU} , z_{TD} , z_{EUC} , respectively, where each C-matrix has an additional parameter that controls the spatial range of autocorrelation for that model, and I is the identity matrix.

SSN models require a stream network, observed water temperatures at discrete locations, and spatially and/or temporally explicit covariates. This model uses the National Stream Internet (NSI) network, which was derived from the NHDPlus dataset and prepared for use with SSNs (Nagel et al. 2015). The observed water temperature data were queried from the NorWeST

database, which consists of temperature logger data collected by numerous agencies and groups and contains over 220,000,000 observations at greater than 22,700 sites throughout the western United States (Isaak et al. 2017). Observed temperature sites that had multiple observations within a day and observations on at least 90% of days within a month were averaged in order to obtain a monthly mean water temperature value which was used within the model. The model fits nine spatial covariates and two temporal covariates. The spatial covariates are elevation (m), canopy (%), slope (m/m), annual precipitation (mm), cumulative drainage area (km²), northing coordinate (km), upstream watershed area that is lake or reservoir (%), the amount of flow that is base flow (%), and tailwater (binary - 0, 1). The majority of these covariates are from NHDPlus, with the exception of base-flow index (developed by Wolock 2003) and northing coordinate and tailwater (determined by Isaak et al. 2017). Each of these covariates was calculated at a 1 km interval, and GIS was used to spatially link these covariates with the stream network. The temporal covariates are air temperature (degrees Celsius) and flow (m³/s). Air temperature was obtained from the NCEP RegCM3 reanalysis in the form of 15 km gridded data (Hostetler et al. 2011). The data were subset to include only grid cells within the spatial extent being modeled. Monthly mean air temperature values were calculated, and these values were linked to water temperature observations by year. Flow time series were queried from the USGS National Water Information System for gages within the spatial extent being modeled. Gaps in the time series were filled using an iterative PCA approach (Josse and Husson 2016). Monthly means were calculated, and these values were linked to water temperature observations by year.

The data were split into a training dataset and a testing dataset, such that approximately 80% of the data were used for model fitting and 20% of the data were used for model validation. When a site had data in multiple years, all data for that site were included in either the training or testing dataset rather than being split between them. Leave-one-out cross validation was also performed on the training dataset, and three metrics were calculated on each the training dataset and the testing dataset to quantify the performance of the model: the square of the correlation coefficient between observations and predictions (r^2), the root mean square prediction error (RMSPE), and the mean absolute prediction error (MAPE). The model fits were used to predict water temperature values at a 1 km resolution for all rivers in the modeled region for the period 2002-2011 using the universal kriging equation which accounts for both the model predictors and spatial autocorrelation (Cressie 1993).

Analyses – spatial and temporal patterns of salmonid thermal exposure

Our goals are to compare life stages by population and run in the context of temperature exposure. Here we examine thermal exposure for Central Valley runs. Monthly mean stream temperatures were extracted for each distribution point in ArcMap. Here, we examine preliminary differences among Central Valley runs. Once stream temperatures are available for every watershed, patterns in thermal exposure will be compared using linear regression and analyses of variance (ANOVAs).

RESULTS

Stream temperature

Currently, we have completed analyses for the regions of central California and Mid-Columbia. Preliminary SSN models for the central California region had a high degree of predictive capability in all months. The leave-one-out cross validation resulted in r^2 values of 0.86 – 0.96, RMSPE values of 0.70 – 1.71, and MAPE values of 0.50 – 1.19 for the central California region. For the Mid-Columbia region, the r^2 values were 0.79 – 0.94, RMSPE values were 0.67 – 1.71, and MAPE values were 0.45 – 0.81. The out-of-sample validation also showed predictive capability of the models, with r^2 values of 0.70 – 0.86, RMSPE values of 1.18 – 2.84, and MAPE values of 0.85 – 2.27 for the central California region; and r^2 values of 0.48 – 0.88, RMSPE values of 0.90 – 2.15, and MAPE values of 0.65 – 1.17 for the mid-Columbia region (Table 1, Fig. 2).

There were clear trends in the covariate effects on water temperature in central California (Fig. 3). Elevation had a strong negative effect in all months; precipitation had a negative effect in most months; air temperature had a positive effect in most months; tailwater had a negative effect in the spring, summer, and fall (April – September) and a positive effect during the winter (November – January); flow had a negative effect in the spring and summer (March – September); and riparian canopy had a negative effect in the summer and fall (June – October). The predicted temperature values for all rivers were mapped (central California temperatures shown in Fig. 4) and were utilized in preliminary statistical analyses examining the thermal regimes of Chinook populations and life stages.

Spatial and temporal patterns

Preliminary results indicate that considerable phenological variation exists within and between populations (Fig. 5, Appendix 1 Table S1.1). For example, Fig. 5 shows that peak spawning for spring run populations occurs August-October, September-October for summer runs (not shown in Fig. 5), and October-December for fall runs. There is not a clear latitudinal cline in peak spawning month. For example, many Pacific Northwest populations spawn during the peak spawning month for Central Valley fall (October) and spring run (September). The only winter run population spawns in May along the Sacramento River.

For spawning Chinook within the Central Valley, spring-run had the broadest thermal exposures and experienced the highest temperature (avg: 14.81°C; range: 10.48-20.27°C), fall-run had the lowest average exposure and narrowest range (avg: 13.08°C; range: 10.96-15.79°C), and winter-run experienced the highest average (avg: 14.83°C; range: 11.94-18.96°C) (Fig. 6). An ANOVA and Tukey HSD analysis revealed that fall-run experience temperatures ~1.7°C cooler than both spring-run ($p = 0.0$) and winter-run ($p = 0.0$), but winter-run and spring-run were not significantly different ($p = 0.99$).

While perhaps unsurprising, these results could have important implications. In the Central Valley, winter-run and spring-run Chinook are declining more rapidly than fall-run. Winter- and spring-runs experience similar, warmer temperatures during spawning compared to fall-run, perhaps contributing to their decline. A broader comparison among other populations throughout the Western U.S. will better elucidate these patterns.

FUTURE WORK

We plan to apply these SSN methods to all regions throughout the western United States with anadromous salmonid populations (Fig. 7). When obtained, monthly stream temperature for all major watersheds containing anadromous Chinook populations will allow for a more complete analysis of thermal and phenological patterns. We expect to show that certain life stages (e.g. spawning) occur over a much narrower range of temperatures than other life stages (e.g. juvenile rearing). This will be the first broad-scale work examining if California populations, including Central Valley, are distinct from Pacific Northwest populations, or if thermal exposure occurs on a latitudinal cline. By defining thermal exposure for each life stage of each population, this work will also provide a baseline for future laboratory studies examining thermal tolerance of different populations.

Q2. Can we improve site-specific temperature management in the Central Valley by using thermal performance curves?

INTRODUCTION

Region 10 criteria provide binary temperature thresholds that managers need to meet in order to protect salmonids, but most of the research involved in setting these thresholds was based on Pacific Northwest populations. In California, water temperature often meets or exceeds these thresholds, especially during years of extreme temperature or drought. For example, in 1977 in the second of two subsequent drought years, water temperatures in the Sacramento River exceeded the requirements of every life stage from July through October (Boles 1988). A 4-year drought from 2012-2016 resulted in high egg mortality of winter- and fall-run when temperatures in the Sacramento River exceeded 16°C (Bland 2015), above the Region 10 threshold 13°C for spawning (U.S. EPA 2003). In instances when temperature requirements cannot be met, the Region 10 binary thresholds do not provide guidance on how cold water resources should be best be managed to minimize negative impacts on salmonid populations. Although there is currently not enough information to assess if new temperature thresholds for California salmonids are needed (Zillig et al. in prep), here we develop a framework using continuous thermal performance curves (TPCs) to quantify thermal effects across life-stages and ultimately help prioritize cold water resources in years when Region 10 criteria cannot be met.

Thermal performance curves quantify the relationship between temperature and performance of a particular process (e.g. survival, growth, reproduction). Laboratory experiments take a direct, explicit approach to quantifying the thermal effects on a trait in a controlled setting by varying a single variable, i.e. temperature, while keeping all other variables (e.g. flow, photoperiod) constant. Modeling the effects of temperature on physiological performance results in a thermal performance curve (TPC) that describes temperature-dependent effects on a trait (Schulte et al. 2011). For example, by relating juvenile growth from 11 Chinook populations to temperature, Perry et al. (2015) defined a TPC that calculates how temperature affects juvenile growth (Fig. 8). TPCs thus define the optimum temperature (the temperature at which performance is maximized) as well as how deviations from the Region 10 thresholds affect performance. If the shape of the TPCs differs substantially among life-stages, then exceeding Region 10 criteria by the same amount can lead to substantially different population impacts. TPCs are therefore ideal to compare temperature-dependent responses across life stages, between populations, and to changing temperatures (Eliason et al. 2011, Zillig et al. in prep).

Here, we develop a framework that provides a quantitative approach for assessing thermal impacts in Central Valley rivers across runs and life stages, illustrated in Fig. 9. Specifically, we examine thermal effects on energy use for adults holding, egg-to-fry survival, and juvenile growth rate using the best temperature-dependent models currently available for Chinook. These TPC models are combined with local distribution and phenology data and stream temperature to translate spatial-temporal temperature data into maps of life stage-specific performance in space and time. Thermal performances across life stages are then compared in a spatial-temporal context to determine which life stages along a river are the most vulnerable to temperatures exceeding the Region 10 thresholds. In years when the Region 10 criteria cannot be

met, this method provides local managers the information to appropriately prioritize cold water resources to minimize the negative thermal impacts on salmonid populations.

METHODS

Overview of framework

The goal of this section of our project is to develop a framework to assess thermal impacts across life stages in different Central Valley rivers. First, we obtain local phenology and distribution data (e.g. from carcass surveys) from a river to determine when and where different life stages occur. Second, water temperature along that river is linearly interpolated from observed temperature values. Next, these temperatures are used as inputs in various stage-specific thermal performance models that relate temperature to physiological performance. The models that we employ are based on the best data currently available for Chinook, but can be updated or changed as better data become available. Finally, thermal effects are compared between life stages to help elucidate which life stages are the most vulnerable to negative thermal impacts. Below, we describe in detail how each of the components of this approach (local distribution and phenology datasets, temperature monitoring data, and TPC models are combined to estimate thermal impacts by applying our framework to the Yuba River.

Datasets

We chose to illustrate our framework on Yuba River as it represents average to moderately good habitat for spring-run Chinook in the Central Valley (Boughton et al. in prep). To examine thermal effects on different life stages at local sites, we need to know where salmon occur for each life stage, when each life stage begins and peaks, and the temperatures associated with these life stages. We used the distribution dataset we aggregated from Q1 to determine spatial locations of life stages along the Yuba River (Fig. 10), but for our final project, we will use higher-resolution, site-specific distributions. Phenology was used to determine the start and peak dates of each life stage, necessary for modeling. Our future applications of the method will make use of site-specific phenology and distribution data that is available in many rivers through ongoing weir, redd, carcass, and screw trap surveys. These distribution and phenology data define which points in space and time we apply the various life-stage-specific TPCs.

To obtain daily stream temperatures over an entire year for all river kilometers, we linearly interpolated actual stream temperature observations to create stream temperatures along a river that match the spatial-temporal resolution (i.e. 1km-daily) of the distribution-phenology data. For our preliminary example, we analyze 29 km of the Yuba River.

Models

Temperature-dependent metabolic expenditure

Sexually immature spring-run chinook adults migrate toward the spawning grounds a few months before spawning is initiated, holding in low-flow pools as their gonads mature and stream temperatures drop (Moyle 2002). During this period, they do not eat (McCullough 1999) and therefore have a finite amount of energy to cover the costs of maintenance metabolism.

Energy use increases exponentially with temperature, so here we employ a temperature-dependent metabolic expenditure model to calculate the energy expended by an adult holding prior to spawning (from Martin et al. 2015):

$$B_{hi} = c_0 M^b e^{DT}$$

where B_{hi} is the maintenance metabolism, or how much energy is used by an adult salmon at a given temperature per unit time. Values for b (-0.217 [unitless]), the mass exponent of maintenance, and D (0.068 [unitless]), the temperature exponent of maintenance, were originally parameterized by Rao (1968) on rainbow trout and were adapted to Chinook in Lake Michigan by Stewart (1980). The c_0 value was parameterized using Chinook data (Martin et al. 2015) and converted to reflect our analyses on a daily time scale ($1572.24 \text{ mgO}_2 \text{ d}^{-1} \text{ kg}^{-1}$). The mass, M , was estimated at 5 kg as in Martin et al. (2015), but this value can be changed if the mean weight of fish in the river is known. Temperature ($^{\circ}\text{C}$), is a value T in space and time, obtained from linear interpolations of observed stream temperatures. After running the model to calculate the maintenance metabolism at a single location in space and time, we summed daily energetic expenditures across time to determine the total energy used per unit mass by an adult holding for n time steps (here, days) at a given location:

$$E_{hTOT} = \sum_{i=1}^n B_{hi} t$$

where n , the number of days holding, was determined by the differential between peak arrival and spawning dates; t represents the time step, in our example, 1 day. From 2004-2010, spring run peak migration along the Yuba River occurred June 29 (YARMT 2014). Peak spawning along the Yuba River for spring run occurs early September to mid-October (YCWA 2013), so we chose the median date of September 24. The differential between the peak migration and median spawning was 87 days, the holding period used in our metabolic expenditure model. Results were converted from $\text{mgO}_2 \text{ kg}^{-1}$ to MJ kg^{-1} ($1 \text{ mgO}_2 = 1.358442 \times 10^{-5} \text{ MJ}$; see Martin et al. 2015). Finally, we calculated the percentage of energy available for spawning allocation as

$$\left(1 - \frac{E_{hTOT}}{E_S - E_M - E_D}\right) * 100$$

where E_S is the starting energy density of a salmon has when migration commences, E_M is the amount of energy used to reach the spawning grounds, and E_D is how much energy remains after spawning upon death. These parameters likely vary to some degree both among populations and years. For our analyses we assumed spring-run start migration with 12 MJ/kg (E_S) (Bowerman et al. 2017a) and use 2 MJ/kg (E_M) during migration (Martin et al. 2015). Post-spawning, salmon carcasses have 4 MJ/kg of somatic energy (E_D), indicating that this energy is unavailable for migration or spawning (Crossin et al. 2004, Bowerman et al. 2017a). Higher percentages indicate that more energy can be allocated toward spawning.

Temperature-dependent embryonic mortality

In the Central Valley, embryos incubate for ~2-4 months prior to emergence (Boles 1988). Survival through the embryonic stage is strongly dependent on temperature (McCullough 1999). We therefore apply a temperature-dependent embryo mortality model based on daily incubation temperatures to calculate the percent mortality of eggs spawned at a given location in space and time (Martin et al. 2017):

$$M_T = 1 - \prod_{i=1}^n \exp(-b_T(T_i - T_{crit}))$$

where M_T is the temperature-dependent mortality throughout the embryonic period, b_T is a parameter defining the slope at which the mortality rate increases with temperature above T_{crit} , T_{crit} is the temperature below which there is no mortality due to temperature, and T_i is the temperature experienced at the i th day of development. The model was parameterized with winter-run Chinook field observations of egg-to-fry survival data, resulting in $T_{crit} = 12.0$ °C and $b_T = 0.024$ °C⁻¹d⁻¹ (Martin et al. 2017). The percent mortality was calculated at each spatial-temporal location.

The time required for eggs to hatch is temperature-dependent (Boles 1988). To determine the length of the embryonic period, n , we implemented the temperature-dependent maturation function by Zueg et al. (2012):

$$1 \leq \sum_{i=1}^n 0.001044 \text{ } ^\circ\text{C}^{-1} \text{ d}^{-1} \times T_i + 0.00056 \text{ d}^{-1}$$

where emergence occurs when the sum reaches 1. For this draft, we assumed a finite incubation length regardless of spawning date. By applying the above model to the average start date of incubation along the Yuba River for spring run (September 24; see above), the average length of the embryonic period from this date was calculated to be 77 days (range: 70-84 days). For the final project, we plan to incorporate a distribution of spawning times to account for temperature-dependent differences in the length of the embryonic period.

Temperature-dependent juvenile growth rate

The ability to successfully smolt is size- and temperature-dependent (Ewing et al. 1979, Healey 1991, McCullough 1999), such that fish with low growth rates may undergo desmoltification, revert to parr, and return to freshwater, resulting in subsequent high juvenile mortality (McCullough 1999). Growth rates of fish are temperature-dependent, and so we apply a juvenile growth model based on temperature (Perry et al. 2015):

$$\Omega = d * (T + T_{corr} - TL) * (1 - \exp(g * (T + T_{corr} - TU)))$$

where Ω = the mass-standardized growth rate (specific growth rate per 1g of fish), T = mean temperature over the growth period, d and g are shape parameters, and T_L and T_U are parameters defining the lower and upper thermal limits at which the growth rate is zero. Perry et al. (2015) parameterized the model with experimental juvenile growth data from multiple Chinook populations, resulting in $d = 0.415$, $g = 0.315$, $T_L = 1.833$ °C, and $T_U = 24.918$ °C. These growth parameters were estimated from laboratory studies with salmon reared in conditions that are likely unrepresentative of conditions in the field (e.g. ad libitum rations), and thus may underestimate thermal impacts. For example Childress and Letcher (2017) found that thermal performance curves for brook and brown trout in the field were reduced by ~2-3°C in the field compared to laboratory studies. Martin et al. (2017) found a similar shift in thermal tolerance for Chinook winter-run embryos from lab to field. Following Childress and Letcher (2017) and Martin et al. (2017), we applied a temperature correction factor, $T_{corr} = 3.0$ °C. The relative growth rate ($100 * \Omega / \Omega_{max}$) was calculated at spatial and temporal locations.

Analyses

We applied each model to the spatial-temporal temperature matrix for the Yuba River in R. Results were graphically illustrated in R using ‘gplots’. To compare thermal effects across life stages, results were converted into percentages. Histograms were then created, where each result in space and time represents one observation. We compared the results from only the points in space and time where each run/life stage occurs.

RESULTS FOR YUBA RIVER

Over the time period from 2003-2004, temperature along the Yuba River ranged from ~8-18°C, with the coolest temperature found upstream during winter, and the warmest temperatures found downstream during summer (Fig. 11A). Preliminary application of our framework to the Yuba River reveals striking differences of the thermal effects on each life stage. Holding Chinook had high energy expenditures downstream during the warmest days of the year (Fig. 11B). Central Valley spring-run tend to hold from about March to September, but high temperatures probably prevent them from holding downstream during the summer. Spring-run Chinook begin migration with approximately 12 MJ/kg, use 2 MJ/kg during migration, and die with approximately 4 MJ/kg (Crossin et al. 2004, Martin et al. 2015, Bowerman et al. 2017a). Therefore, spring-run Chinook with no holding costs would have 6 MJ/kg of energy to allocate to spawning, and individuals that use ≥ 6 MJ/kg will not successfully spawn. Our preliminary results (Fig. 11B) show that all spring-run Chinook salmon would spend a significant amount of energy reserves during the holding period. Our model predicted that spring run typically spend an average of 3.23MJ/kg with a maximum of 4MJ/kg to hold for a 77 day period. For reference, our model predicts that a salmon holding in 12°C water for the same length of time would spend 3.03MJ/kg holding. Assuming the spring run begin the holding period with 6MJ/kg of surplus energy for holding and reproduction, our model predicts that spring run in the Yuba River would have an average of 7% and maximum of 32% less energy available to allocate to reproduction compared to a reference population holding at 12°C. Assuming a mean egg weight of 300mg and an egg energy density of 10MJ/kg, a 5kg female salmon in the Yuba River would have enough

energy to produce ~4,600 eggs (minimum ~3,300 eggs) relative to the 5,000 eggs produced by a female holding at 12°C.

Given an incubation time of 77 days, Fig. 11C reveals the percent mortality of eggs spawned at each location in space and time. The model predicts low temperature-dependent mortality during much of the time that fall-run fry are spawned. Spring-run that spawn early in the season experience higher egg mortality than those that spawn during the peak or later. Fall-run tend to have relatively low egg mortality along the Yuba River. Note, however, that this preliminary analysis does not include the full distribution of fall-run along the Yuba River.

Juveniles have the highest thermal tolerance range of all Chinook life stages. Sill, high temperatures can inhibit smoltification or directly cause death by impairing metabolic activity, deterring feeding, reducing swimming ability, and triggering the production of heat shock proteins (McCullough 1999). However, temperatures along the Yuba River from 2003-2004 never exceeded 18°C, and thus the TPC model for growth – even with a 3C safety factor -- predicts that juveniles are unlikely to experience reduced growth due to elevated temperatures at any location in space and time (Fig. 11D). Thus, in the Yuba River for these years, water temperatures are likely sufficient to support both stream-type and ocean-type rearing strategies.

Comparing the temperature-dependent effects between life stages reveals important differences (Fig. 12). Juveniles are predicted to experience high growth rates at all spatial temporal locations. Similarly, most adults holding will successfully spawn. In contrast, there was predicted high egg mortality, indicating that the ability to successfully spawn and emerge may be more limiting in this river than juvenile growth. In this case, managers should focus on enlarging or maintaining suitable habitat for spawners and ensuring that stream temperature remains appropriate during the full incubation period.

We also find important differences between populations. Spring-run experience higher egg mortality than fall-run because they spawn earlier in the year when temperatures are warmer. One potential reason for this is that spawning later would require spring-run salmon to hold for even longer periods, which would reduce energy available for reproduction and risk pre-spawning mortality due to starvation. Historically, spring-run spawned at cooler temperatures, but much of that habitat has been blocked by dams. In the Yuba River, spring-run are limited by the impassible Englebright Dam. If temperatures warm near the mouth of the Yuba River, spring-run spawning grounds will continue to shrink. As this population is endangered, managers can use the preliminary results from our study to show that cooler temperatures during the extreme dates of spawning will increase egg-to-fry survivability, potentially increasing the population size.

FUTURE WORK

Our preliminary results are based on 29 km of the Yuba River, but we plan to extend our analysis from the Feather River to Englebright Dam. We also incorporated coarse-scale distribution and phenology data for our preliminary analysis, but our final work will include site-specific data.

We plan to expand this framework to analyze two other inhabited rivers in the Central Valley. Taking into consideration Chinook run timing and size, along with data availability and

spatial distribution, we suggest additional modeling effort be focused on the Tuolumne and Stanislaus Rivers. These rivers are regulated by hydroelectric dams, allowing for a controllable response if an optimal scenario is found. The Yuba River still has a spring run population so alterations in flow regimes could directly benefit the recovery of this run. Spring run fish have returned to the main stem San Joaquin for the first time in 60 years due to flow increases; the Tuolumne and Stanislaus historically had spring run populations, so flow alteration could possibly help other populations reestablish as well. Our full list of 22 candidate streams located in the California Central Valley may be found in Appendix 2 Table S2.1. These streams range in size and complexity but all contain populations of anadromous Chinook salmon.

We also plan to model non-regulated streams as a baseline comparison for how streams in the Central Valley would naturally function without large dams. This will allow us to model natural hydrograph TPCs which may be informative on how dam operators could alter flow regimes. As a way to establish baseline models for natural flows, we plan to examine Mill Creek in the Sacramento River watershed and the Cosumnes River. Mill Creek is one of the best remaining habitats for salmon in the north side of the valley, and the Cosumnes River is the largest unregulated river in the southern portion of the Central Valley. Locations of our suggested rivers are found in Fig. 10.

Q3. Additional studies needed to develop site-specific thermal criteria

If distribution, phenology, and stream temperature are known, our framework illustrated above is easily applied to other rivers, populations, or salmonid species, with appropriate model modifications. Our method paves the way for future studies to validate and improve current models, incorporate additional models, and develop a full life cycle model. Above, we used our framework to compare direct thermal effects on life stages within a single river over the course of two years, but analyses could be expanded in a variety of ways. Below, we discuss each of these topics.

VALIDATION AND IMPROVEMENT OF MODELS

Laboratory and/or field studies specific to Central Valley Chinook may improve parameter values of these models and therefore the application of this framework to Central Valley predictions. The models we applied to Central Valley populations are the current best available for Chinook, but the models were not always parameterized with Central Valley salmon, or even Chinook. The metabolic expenditure model uses some parameters (b and D) from Stewart (1980), who based his Chinook metabolism model on rainbow trout data (Rao 1968) because there was so little information for Chinook, and Chinook and rainbow trout (steelhead) have similar life histories and are of similar sizes. This model also calculates how much energy an adult holding uses, but does not quantify changes in fecundity or temperature-dependent pre-spawn mortality; research is needed in this area for natural-origin fishes (Bowerman et al. 2017b). We use a juvenile growth model developed from laboratory results from multiple Chinook populations, but only one population was from in the Central Valley (Perry et al. 2015). Field studies of temperature-dependent juvenile growth rates from multiple populations in the Central Valley would determine how effective this model is for these populations. The egg mortality model was parameterized using Central Valley winter-run chinook (Martin et al. 2017), but other runs may result in slightly different parameter values.

Field studies are needed to improve and validate some laboratory-based models. For example, Martin et al. (2017) found differences in thermal impacts on winter-run egg mortality in laboratory and field contexts, probably stemming from unrealistic laboratory conditions. The metabolic expenditure model is based on laboratory results for rainbow trout, and field studies focusing on Chinook adult metabolism are necessary (but see Bowerman et al. 2017a, 2017b).

Juvenile growth rate is temperature-dependent, but also depends on food availability (McCullough 1999). The model used here (Perry et al. 2015) was based on laboratory studies where juveniles were fed ad libitum, but feeding at 60% satiation results in growth rates of ~80% of maximum (McCullough 1999). If food availability in a system is known or estimated, a parameter can be applied to the juvenile growth model. Mark-recapture studies are ideal to develop field-calibrated TPC models of growth rate, such as Childress and Letcher (2017), and more field studies are needed to assess the relationship between juvenile growth, temperature, and food availability. In conclusion, field and laboratory studies on Central Valley populations are lacking compared to Pacific Northwest studies (Zillig et al. in prep), and much research is needed to validate and improve these models for Central Valley populations.

ADDITIONAL MODELS AND FULL LIFE-CYCLE MODEL

Our framework may be used to guide future research relating temperature to other types of performance, including disease mortality and behavior, and the influence of other factors on performance, such as food availability and dissolved oxygen. For example, some salmonid diseases result in increased mortality at higher temperatures. Although some temperature-dependent mortality models are available, they assume unrealistic conditions such as 100% initial infection rates, or are based on non-natural scenarios like densely packed juveniles rearing in hatcheries. Field studies of disease prevalence and mortality in natural populations are required to link laboratory results to natural conditions.

As applied here, our framework assumes that fish are remaining in the same spatial location over time, but temperature can directly and indirectly influence fish behavior. Adults and juveniles can alter directly alter their behavior to buffer their exposure to elevated temperatures (McCullough 1999). Site-specific studies on the use of cold water pools through a range of temperatures can help elucidate behavioral thermoregulation. A behavior model could then be incorporated into the framework to define temperature-dependent changes in phenology or distribution. Indirectly, high temperatures may result in greater mortality due to predation as many predators thrive at warmer temperatures than salmonids. GPS tags on juveniles can help determine predation rates at spatial and temporal localities. A TPC showing juvenile mortality likelihood due to predation across temperatures could be incorporated.

Temperature influences metabolism, such that stressed fishes expend more energy, and temperature also influences the amount of dissolved oxygen, such that higher temperatures hold less dissolved oxygen. Aerobic scope studies calculate the difference in oxygen uptake of a fish at rest and during exertion (Clark et al. 2013). By relating aerobic scope results of a life stage (e.g. adult holding) to a range of temperatures in a TPC, models can be added to our framework that show the relationship between temperature, energy, and dissolved oxygen (Zillig et al. in prep).

As new TPCs are developed for other temperature-dependent processes (e.g. temperature-dependent mortality due to disease, temperature-dependent growth rates at specific food levels, etc.), these models could be incorporated to this framework. Although beyond the scope of this project, ultimately these and other models can be linked through a full temperature-dependent life-cycle model. In that way, thermal effects on different life-stages can be compared in common currency: population growth rate. Because some TPCs measure effects that are not directly connected to population level effects (e.g. energy expenditure, growth rates), work is needed to quantify how each of these currencies translates to effects on demographic rates (survival and reproduction rates).

EXPANSION OF FRAMEWORK – FUTURE APPLICATIONS

A primary goal of our framework is to provide managers with information to enact measures to mitigate negative thermal effects. Using our method, managers can assess current thermal suitability along rivers to determine when and where cooler water could help reestablish populations or increase abundance. For example, Fig. 11C shows high egg mortality toward the downstream section of the river. Cold water increases could increase the amount of suitable

thermal habitat, reducing egg mortality and potentially increasing population growth. If stream temperature is available at fine scales, these models could be applied to assess the locations and connectivity of potential thermal refugia utilized by holding adults (Fullerton et al. 2017). Managers could use this information to potentially create more refugia, resulting in adults expending less energy during holding and allocating more energy to spawning.

We illustrated the application of our framework to determine thermal effects over a two-year time span, but annually repeated surveys can reveal how phenology and/or distribution changes help to buffer against temperatures during warm years. If long-term data on phenology and distribution are available, this method can be used to predict behavior based on thermal habitat suitability. For example, adults may hold longer when temperatures are warmer than average, spawning later, or move upstream to cooler pools. Juvenile rearing strategies are partially temperature-dependent (Brannon et al. 2004), and our juvenile growth model can predict the growth rates of juveniles that outmigrate soon after emergence (ocean-type) or rear for a year or more (stream-type). For populations that have both rearing strategies, this model can be used to determine which type will be more prevalent year to year, or determine how long juveniles will rear if initial size and size needed to outmigrate are known, potentially affecting management. Future stream temperature forecasts allow for estimates of changes in distribution and phenology of different life stages, and our method allows comparison between life stages. Ultimately, application of our framework allows for more accurate conservation planning and management of these economically important yet declining salmonids.

CONCLUSIONS

Our study will ascertain how the thermal exposure of Central Valley populations fits within the broad geographic extent of all West Coast populations, the first step in statistically calculating if and how Central Valley populations differ in thermal exposure. If populations do differ, the next step will be determining if Region 10 criteria are still applicable to populations in California. If Region 10 criteria are not appropriate for salmonids in warmer environments, multiple laboratory and field studies are necessary to develop new criteria for California populations (see Zillig et al. in prep). However, these studies and analyses will take years. In the meantime, our framework using thermal performance curves allows managers to determine the best way to allocate water resources for their specific river when Region 10 criteria cannot be met, and provides more information than a single threshold value. Our framework is incredibly flexible, allowing for future additions or changes as more information is made available. Further, the data needed are knowledge of the distribution, phenology, and associated stream temperatures, and this information is already readily available for many rivers, making our framework easily implementable.

LITERATURE CITED

- Bland, A. 2015. For California Salmon, Drought And Warm Water Mean Trouble. YaleEnvironment360. Yale School of Forestry & Environmental Studies. Accessible at <https://e360.yale.edu/features/for_california_salmon_drought_and_warm_water_mean_trouble?utm_source=folwd.com>.
- Boles, G. L. 1988. Water temperature effects on chinook salmon (*Oncorhynchus tshawytscha*) with emphasis on the Sacramento River: a literature review. California Department of Water Resources, Northern District.
- Boughton, D.A., S. John, C.J. Legleiter, R. Richardson, and L.R. Harrison. In prep. On the Capacity of upper Tuolumne and Merced Rivers for Reintroduction of Steelhead and Spring-run Chinook Salmon.
- Bowerman, T. E., Pinson-Dumm, A., Peery, C. A., & Caudill, C. C. 2017a. Reproductive energy expenditure and changes in body morphology for a population of Chinook salmon *Oncorhynchus tshawytscha* with a long distance migration. *Journal of fish biology* 90(5): 1960-1979.
- Bowerman, T., Roumasset, A., Keefer, M. L., Sharpe, C. S., & Caudill, C. C. 2017b. Prespawn mortality of female Chinook Salmon increases with water temperature and percent hatchery origin. *Transactions of the American Fisheries Society*, (just-accepted).
- Brannon, E. L., Powell, M. S., Quinn, T. P., & Talbot, A. 2004. Population structure of Columbia River Basin Chinook salmon and steelhead trout. *Reviews in Fisheries Science* 12(2-3): 99-232.
- Childress, E. S., & Letcher, B. H. 2017. Estimating thermal performance curves from repeated field observations. *Ecology* 98(5): 1377-1387.
- Crossin, G. T., Hinch, S. G., Farrell, A. P., Higgs, D. A., Lotto, A. G., Oakes, J. D. & Healey, M. C. 2004. Energetics and morphology of sockeye salmon: effects of upriver migratory distance and elevation. *Journal of Fish Biology* 65: 788–810.
- Eliason, E.J. & Farrell, A.P. 2014. Effect of hypoxia on specific dynamic action and postprandial cardiovascular physiology in rainbow trout (*Oncorhynchus mykiss*). *Comp. Biochem. Physiol. Part A* 171: 44–50.
- Ewing, R.D., S.L. Johnson, H.J. Pribble, and J.A. Lichatowich. 1979. Temperature and photoperiod effects on gill (Na + K)-ATPase activity in chinook salmon (*Oncorhynchus tshawytscha*). *J. Fish. Res. Board Can.* 36: 1347-1353.

- Fullerton, A.H., Lawler, J.J., Lee, S.-Y., Torgersen, C.E. 2017. Incorporating Spatial Heterogeneity in Temperature into Climate Vulnerability Assessments for Coastal Pacific Streams. Final Report to the North Pacific Landscape Conservation Cooperative.
- Healey, M.C. 1991. Life history of chinook salmon (*Oncorhynchus tshawytscha*). In Groot and Margolis (eds.) Pacific Salmon Life Histories. University of British Columbia Press, Vancouver, BC. pp. 311-394.
- Martin, B. T., Nisbet, R. M., Pike, A., Michel, C. J., & Danner, E. M. 2015. Sport science for salmon and other species: ecological consequences of metabolic power constraints. *Ecology letters* 18(6): 535-544.
- Martin, B.T., A. Pike, S.N. John, N. Hamda, J. Roberts, S.T. Lindley, and E.M. Danner. 2017. Phenomenological vs. biophysical models of thermal stress in aquatic eggs. *Ecology Letters* 20: 50-59.
- McCullough, D. A. 1999. *A review and synthesis of effects of alterations to the water temperature regime on freshwater life stages of salmonids, with special reference to Chinook salmon*. US Environmental Protection Agency, Region 10. pp. 1-291.
- Moyle, P.B. 2002. Salmon and Trout, Salmonidae - Chinook Salmon, (*Oncorhynchus tshawytscha*) in Inland Fishes of California. Los Angeles, California: University of California Press. pp. 251-263.
- Perry, R. W., Plumb, J. M., & W Huntington, C. 2015. Using a Laboratory-Based Growth Model to Estimate Mass-and Temperature-Dependent Growth Parameters across Populations of Juvenile Chinook Salmon. *Transactions of the American Fisheries Society* 144(2): 331-336.
- Poletto, J.B., D.E. Cocherell, S.E. Baird, T.X. Nguyen, V. Cabrera-Stagno, A.P. Farrell, and N.A. Fangue. 2017. Unusual aerobic performance at high temperatures in juvenile Chinook salmon, *Oncorhynchus tshawytscha*. *Conservation Physiology* 5(1): cow067; doi:10.1093/conphys/cow067.
- Schulte, P.M., Healy, T.M. & Fangue, N. A. 2011. Thermal performance curves, phenotypic plasticity, and the time scales of temperature exposure. *Integr. Comp. Biol.* 51: 691–702.
- Stewart, D.J. 1980. Salmonid predators and their forage base in Lake Michigan: a bioenergetics-modeling synthesis. University of Wisconsin-Madison.
- U.S. Environmental Protection Agency. 2003. *EPA Region 10 Guidance for Pacific Northwest State and Tribal Temperature Water Quality Standards*. EPA 910-B-03-002.
- Yuba County Water Agency. 2013. ESA/CESA-Listed Salmonids Downstream of Englebright Dam, Technical Memorandum 7-8. Yuba River Development Project, FERC Project No. 2246.

- Yuba Accord River Management Team. 2014. Feather-Yuba River Interactions with an emphasis on Spring-Run Chinook Salmon. Lower Yuba River 6th Annual Symposium.
- Zillig, K.W., Lusardi, R.A., and N.A. Fangue. In prep. Variation in Thermal Eco-physiology among California Salmonids: Implications for Management.
- Zeug, S. C., Bergman, P. S., Cavallo, B. J., & Jones, K. S. 2012. Application of a life cycle simulation model to evaluate impacts of water management and conservation actions on an endangered population of Chinook Salmon. *Environmental Modeling & Assessment* 17(5): 455-467.

FIGURES AND TABLES

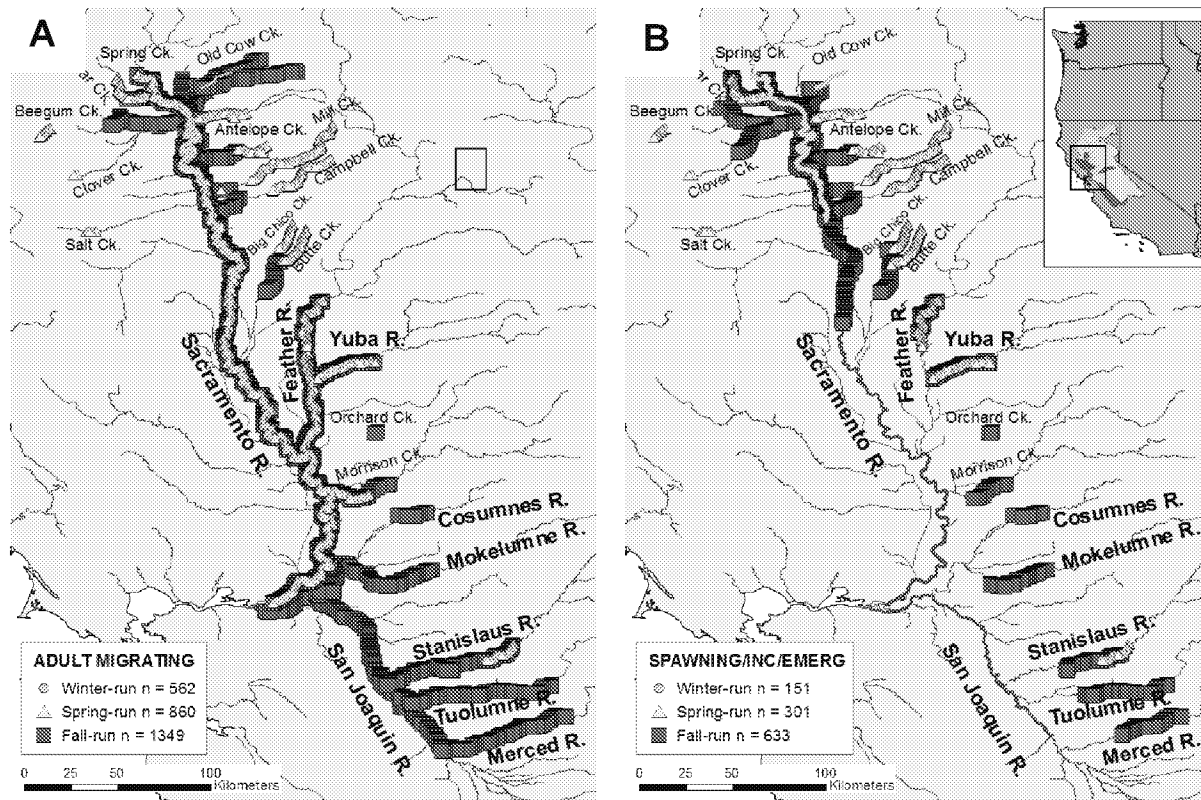


Figure 1. Spatial distribution of Central Valley Chinook by ESU and life stage, with A) showing adults migrating and B) showing spawning/incubation/ emergence. Note that spawning, incubation, and emergence occurrences vary by month but not spatial location.

Table 1. Number of temperature observations (T_{wn}), predicted r^2 , root mean square prediction error (RMSPE) and mean absolute prediction error (MAPE) for each month (1993-2011) for the training dataset (in-sample) and testing dataset (out-of-sample) for the SSN model of: (a) central California region, and (b) Mid-Columbia region.

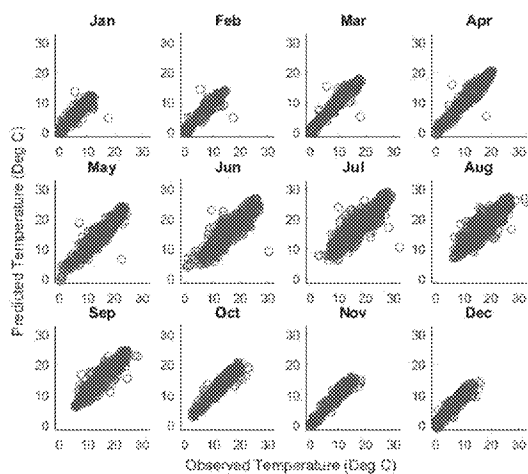
(a)

Month	In-sample				Out-of-sample			
	T_{wn}	r^2	RMSPE	MAPE	T_{wn}	r^2	RMSPE	MAPE
January	1158	0.93	0.85	0.53	278	0.81	1.22	0.85
February	1171	0.95	0.79	0.50	289	0.86	1.18	0.87
March	1178	0.95	0.92	0.62	291	0.86	1.45	1.17
April	1212	0.94	1.00	0.69	295	0.83	1.75	1.44
May	1282	0.90	1.33	0.94	323	0.78	2.12	1.70
June	1645	0.86	1.71	1.19	406	0.76	2.42	1.89
July	2087	0.87	1.69	1.11	515	0.70	2.84	2.27
August	2295	0.90	1.41	0.92	570	0.75	2.54	1.97
September	2014	0.93	1.12	0.74	501	0.81	1.93	1.48
October	1458	0.95	0.86	0.59	360	0.82	1.40	0.97
November	1202	0.96	0.70	0.48	297	0.82	1.28	0.97
December	1141	0.95	0.82	0.59	284	0.74	1.50	1.09

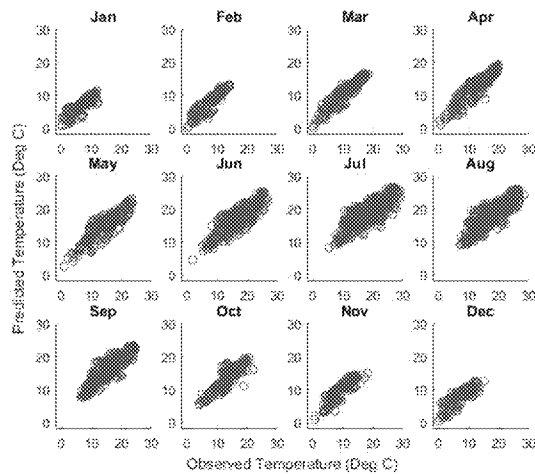
(b)

Month	In-sample				Out-of-sample			
	T_{wn}	r^2	RMSPE	MAPE	T_{wn}	r^2	RMSPE	MAPE
January	973	0.79	0.78	0.49	248	0.57	1.59	0.93
February	993	0.83	0.79	0.50	255	0.72	0.90	0.65
March	995	0.83	0.90	0.51	249	0.81	0.90	0.68
April	1079	0.93	0.67	0.45	271	0.48	1.74	1.04
May	1724	0.91	0.92	0.65	434	0.88	1.09	0.81
June	3635	0.82	1.50	0.81	908	0.83	1.47	1.08
July	6385	0.81	1.71	0.79	1596	0.74	2.15	1.17
August	7434	0.82	1.63	0.69	1858	0.75	1.87	1.08
September	5528	0.94	0.75	0.48	1380	0.82	1.52	0.77
October	2234	0.91	0.91	0.50	559	0.82	1.18	0.79
November	1244	0.92	0.82	0.53	311	0.81	1.18	0.79
December	1071	0.85	0.88	0.54	270	0.61	1.42	0.78

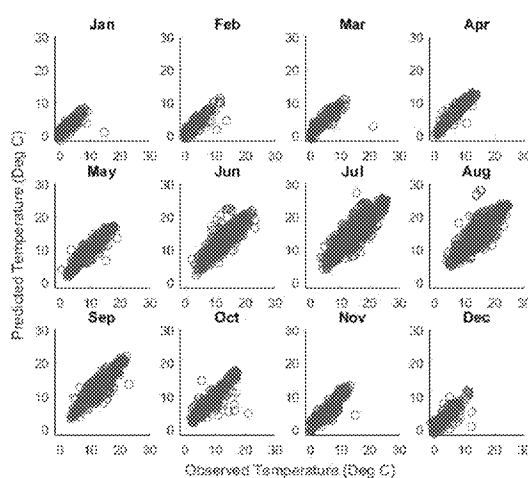
(a)



(b)



(c)



(d)

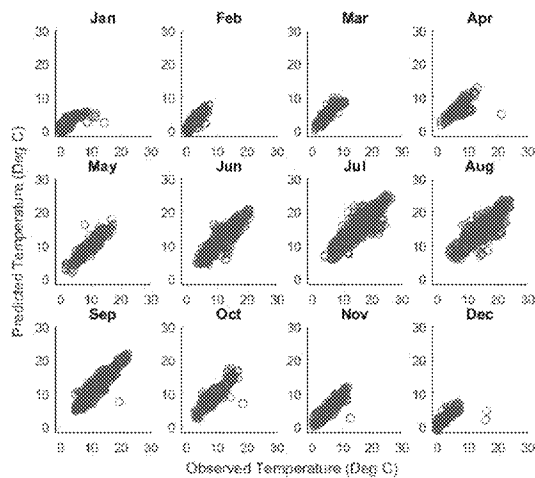


Figure 2. Observed and predicted water temperature values for 1993-2011 for: (a) Central California training data, (b) Central California testing data, (c) Mid-Columbia training data, and (d) Mid-Columbia testing data.

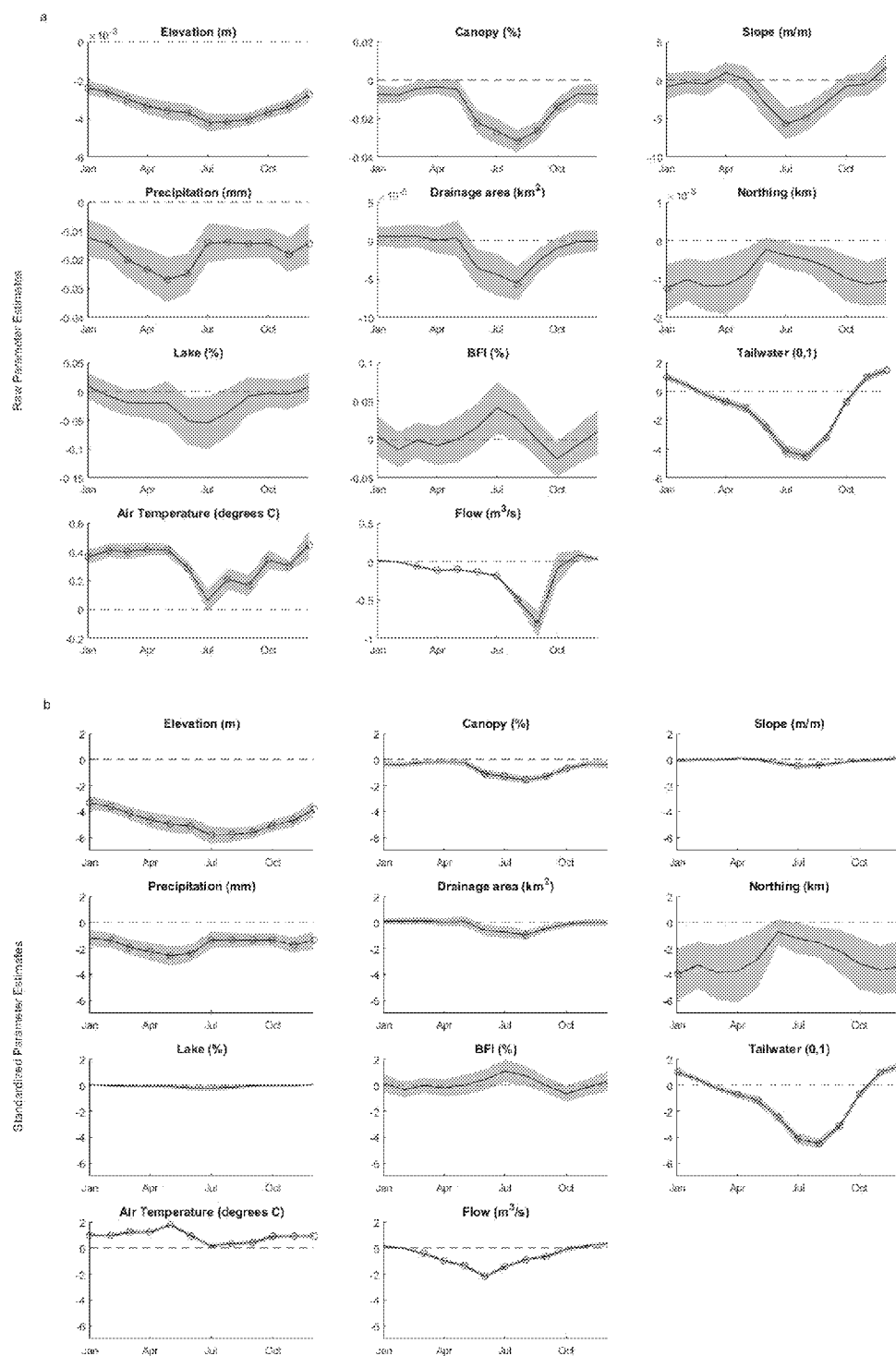


Figure 3. Raw parameter estimates (a), and standardized parameter estimates (b) for all model covariates in all months. Solid line shows the parameter estimate and shaded region shows ± 1 standard error. Red circles indicate covariates that had a significant effect ($p < 0.05$).

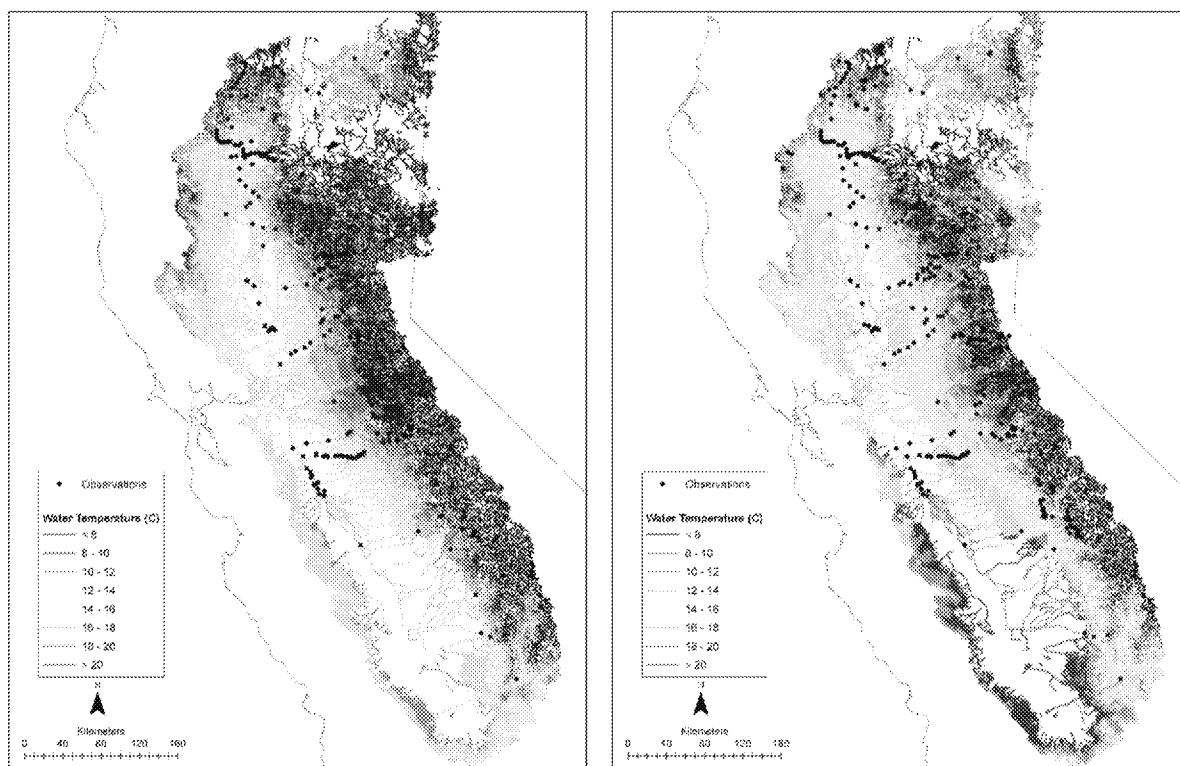


Figure 4. Preliminary predicted water temperature values for the central California region for 1993-2011 for April (left) and October (right).

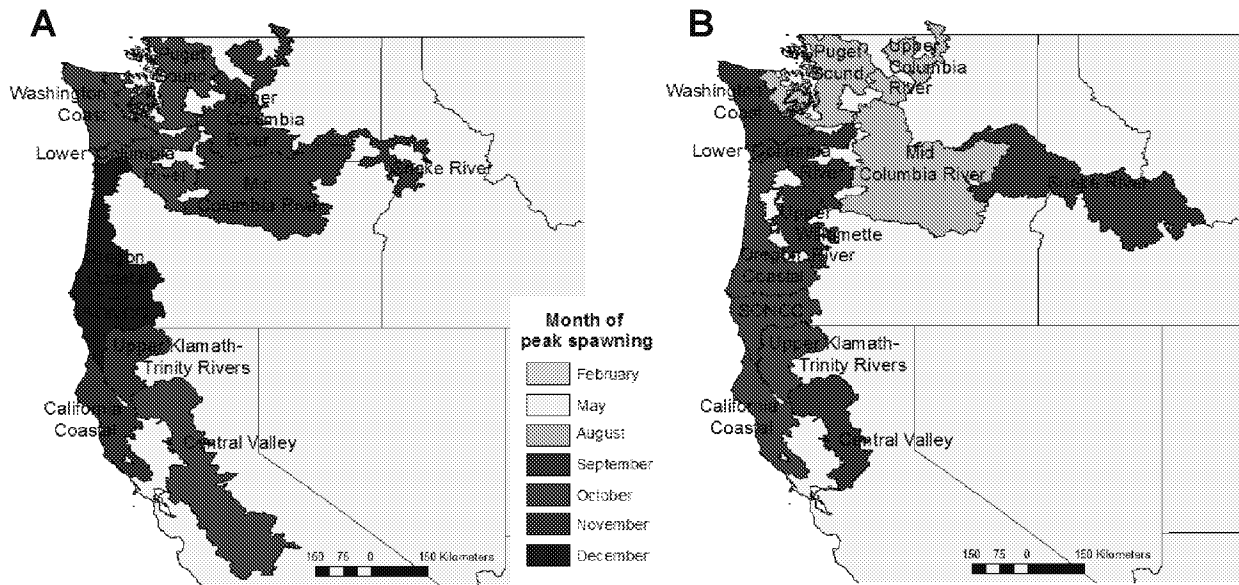


Figure 5. Month of peak spawning of A) fall- and B) spring-run Chinook populations. ESUs were split by run to show differences in phenology. Note that CA Coastal spring-run is extinct, and S. Oregon & N. California Coastal (SONCC) spring-run is mostly extinct.

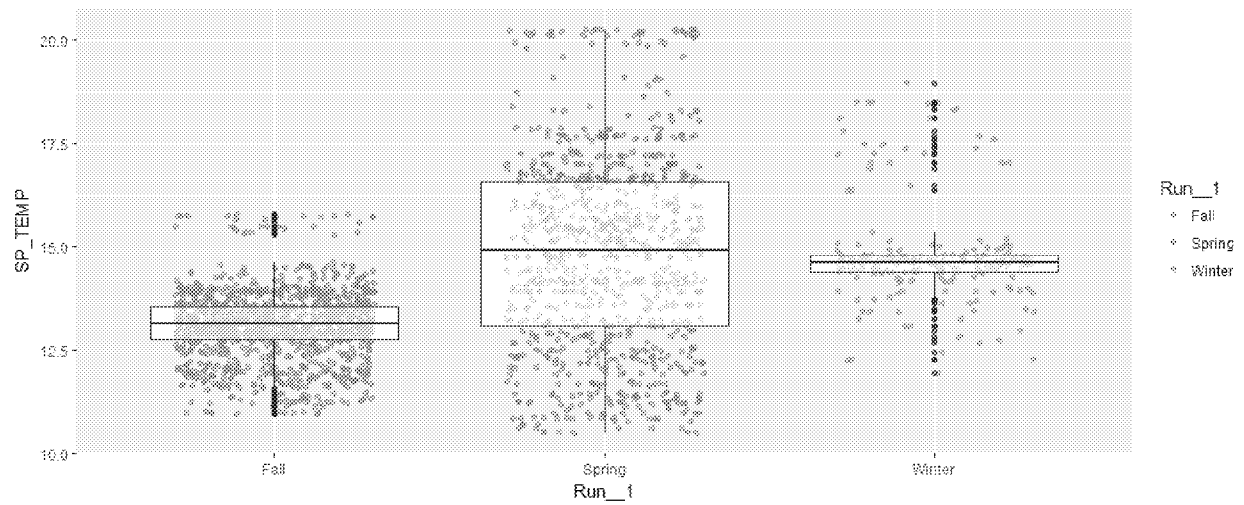


Figure 6. Comparison of the thermal exposures of Chinook spawners by run in the Central Valley. The boxplots show the median, upper and lower quartiles, and outliers. The dots show the thermal exposure of each spawning occurrence.

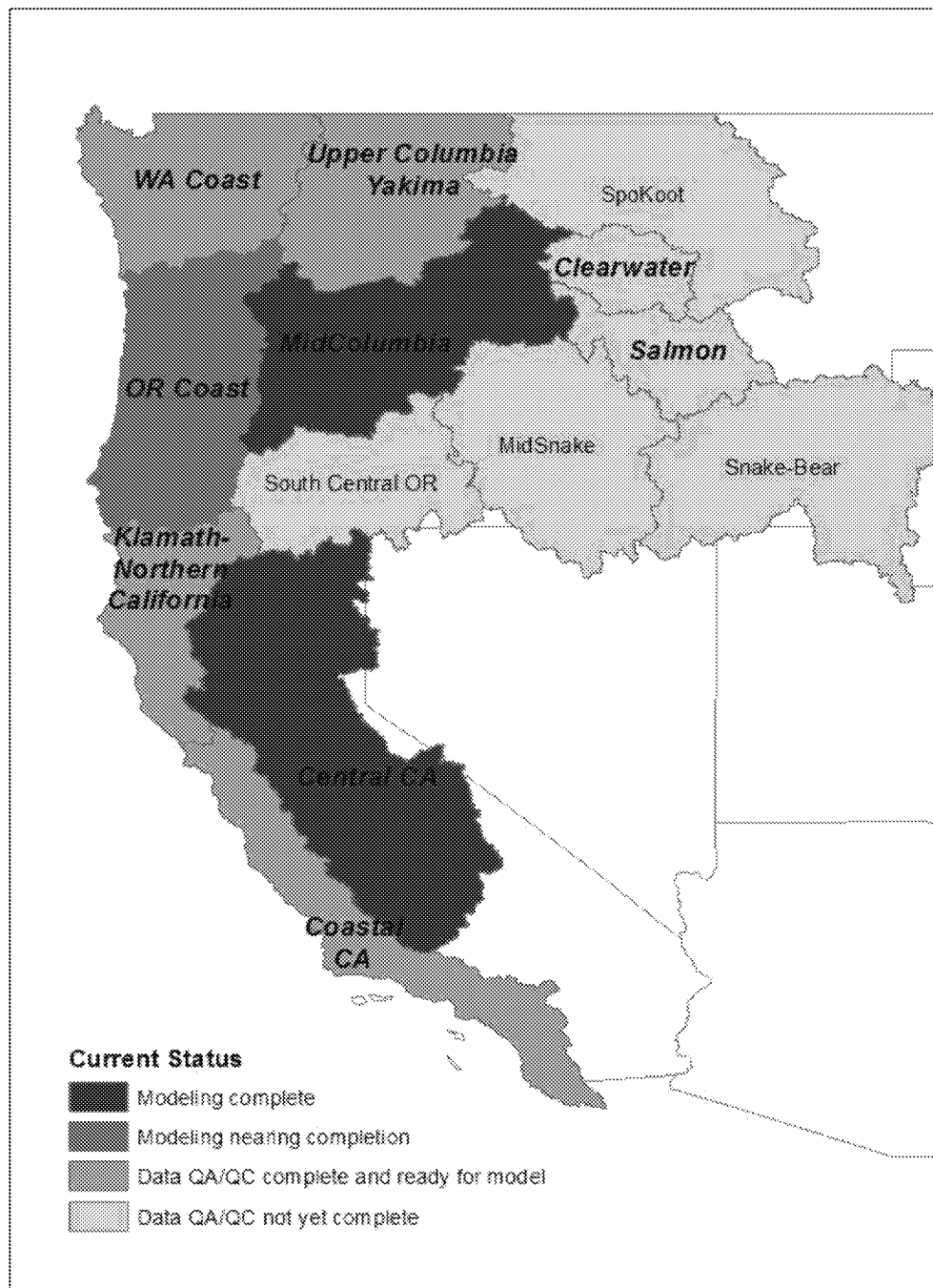


Figure 7. Status of stream temperature modeling project. Modeling has been completed for two regions. Data is currently unavailable (as of 15 July 2018) for six regions, but note that only the Clearwater and Salmon regions (bolded) are important for anadromous salmonids.

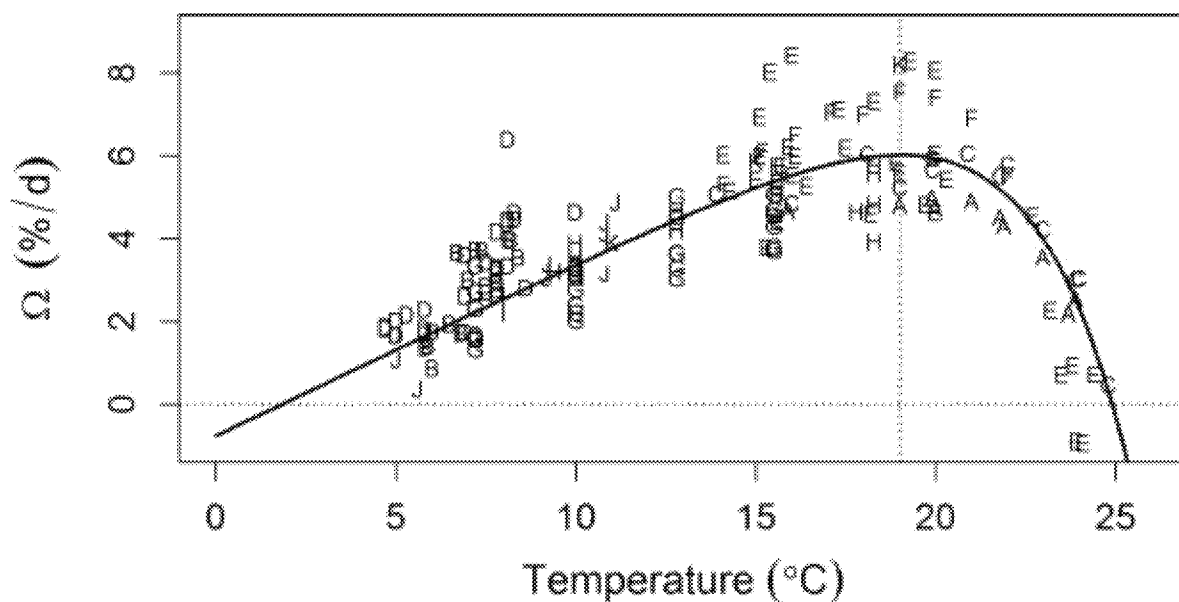
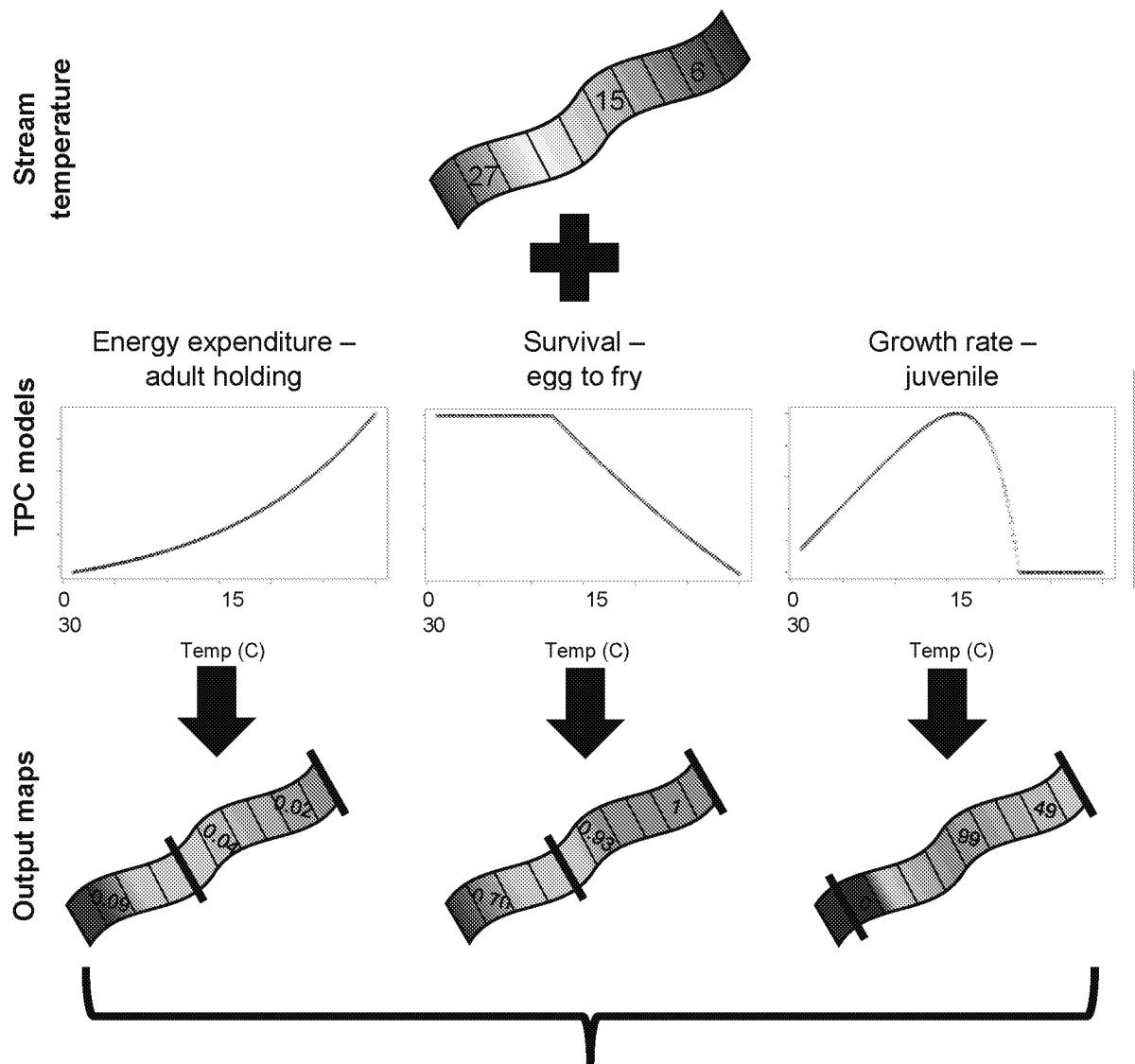


Figure 8. Thermal performance curve for Chinook juvenile growth, from Perry et al. (2015). Using data from 11 Chinook populations (represented by letters), Perry et al. (2015) parameterized this TPC, showing how varying temperatures affect juvenile growth. The optimum temperature at which growth is maximized (vertical dashed line) is 19°C. We apply this TPC in our framework with a field correction factor of 3°C because this study was based on laboratory results (see text).



Comparison of thermal effects of life stages

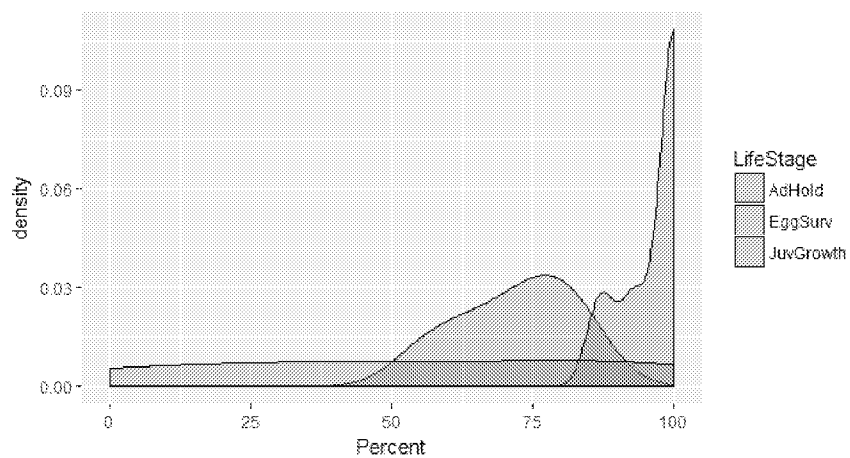


Figure 9. Framework for assessing thermal impacts of life stages along a river using example stream temperatures for a single day. Each thermal performance curve model is run at each spatial location, with temperature (top panel) as the input. The output maps show temperature-based performance, with the limits of the distribution of each life stage bolded. Thermal effects are then compared between life stages (bottom panel) via conversion to a common currency, percent effect: 1) energy expenditure of adults holding is calculated as the percent of energy left to allocate to spawning; 2) eggs surviving to fry is converted to a percentage; 3) juvenile growth rate is the percentage of maximum growth. Note that the kernel density plot is comparing the actual distributions of each life stage (i.e. values within the bolded limits), not the entire river. In this one-day example, there are several locations where juveniles do not grow (0%), but adults holding and egg-to-fry survival perform highly where they are located, indicating that juveniles rearing may be more limiting. For actual data, comparisons are based on multiple days (see text).

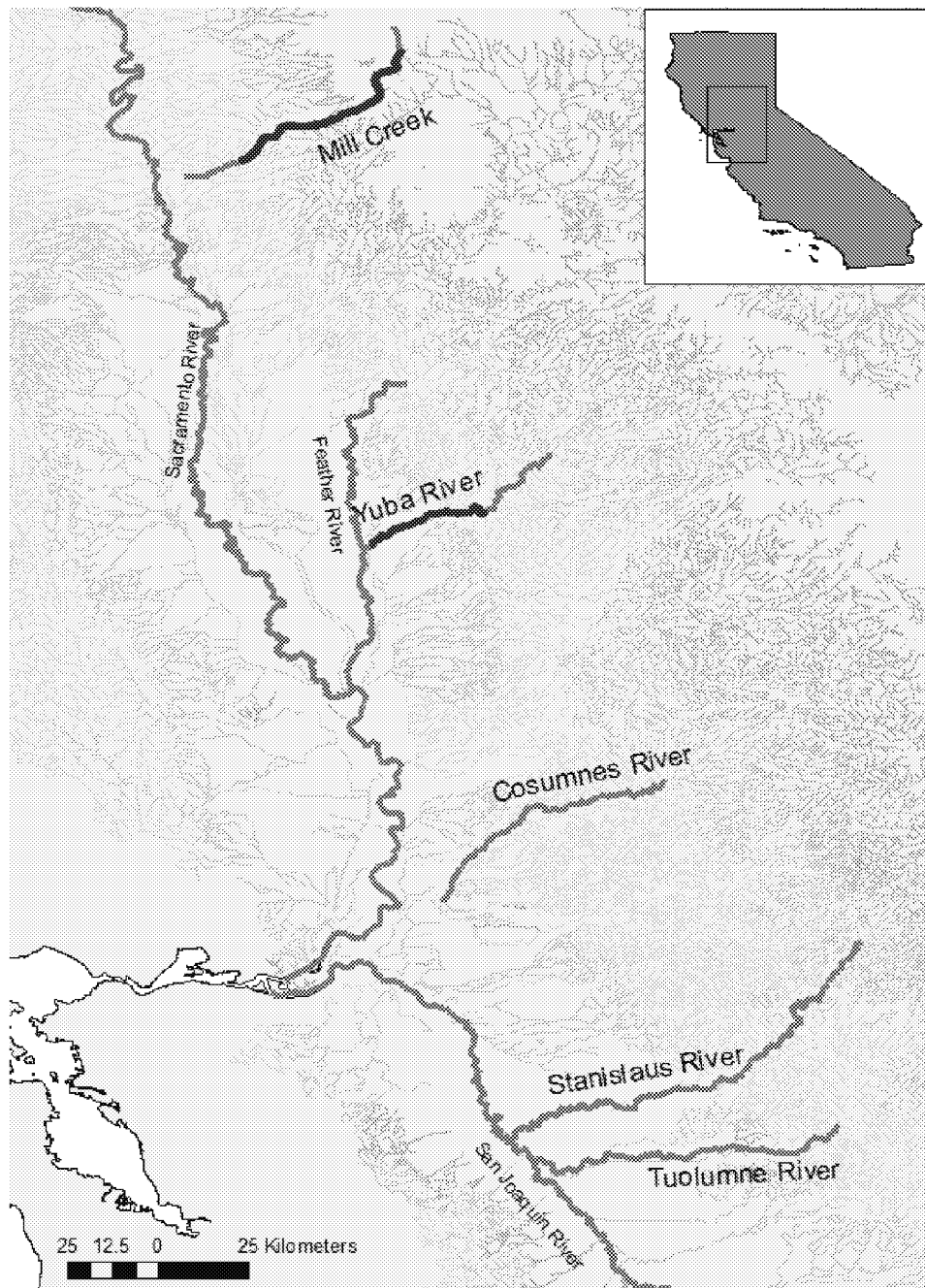
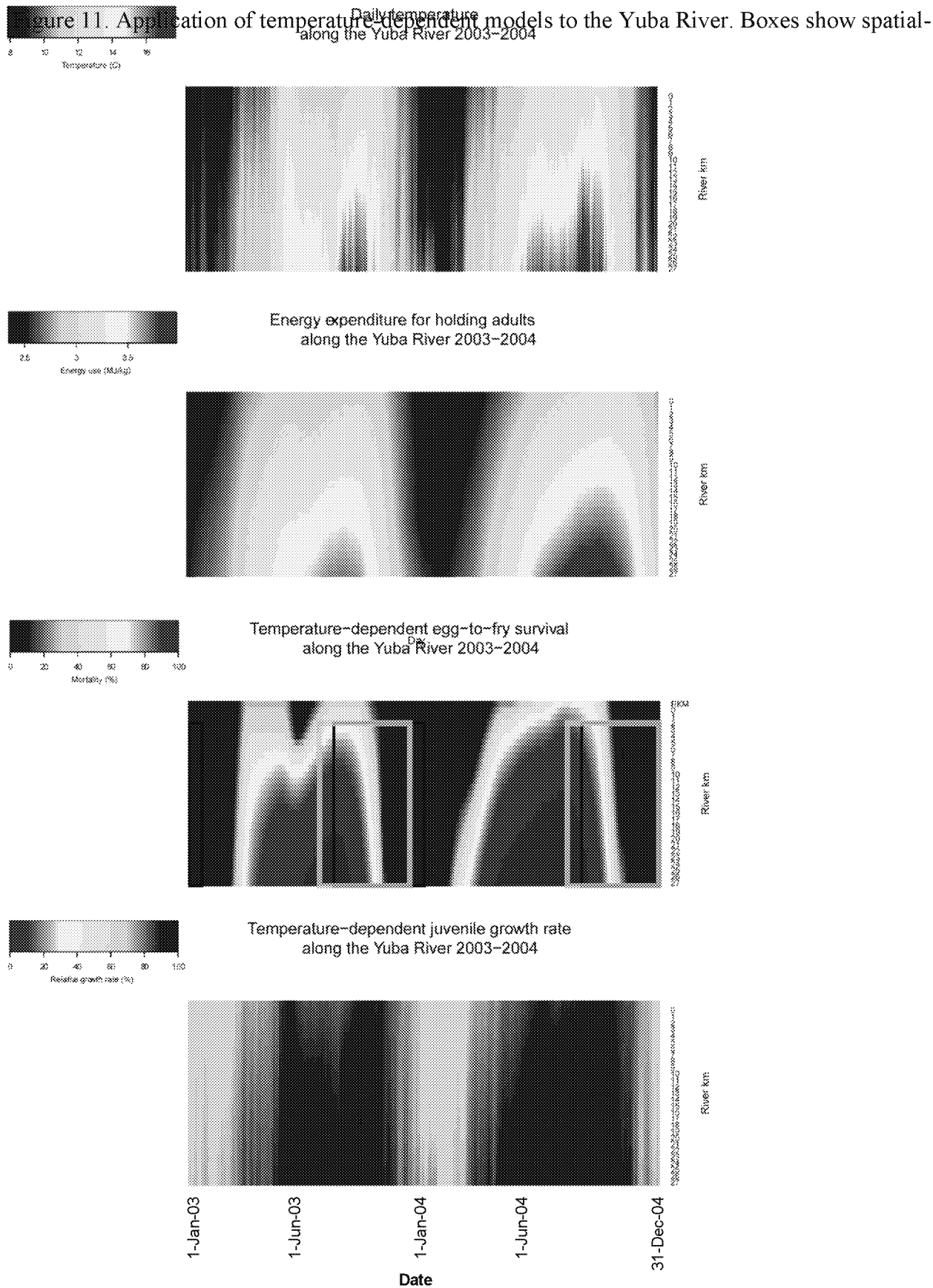


Figure 10. Locations of suggested rivers, and spring run spawning distribution (red). All five prospective rivers have fall run. Spring run were extirpated along the Tuolumne and Stanislaus Rivers. Rivers are shown against a backdrop of Central Valley stream temperatures (preliminary results) for September, the peak month of spawning for spring run. Temperatures range from 9.8°C (blue) to 26°C (red).



temporal distribution of spring-run (gray) and fall-run (black). A) Temperature along the Yuba River from 2003-2004. B) Metabolic expenditure of spring-run adults during the holding period (87 d) along the Yuba River. Each pixel indicates that an adult that holds for 87 days beginning at that point in time and space will expend the calculated amount of energy. C) Egg-to-fry survival given an incubation length of 77 days. Each location in space and time (pixel) indicates that percentage of eggs spawned at that spatial location that would experience mortality. D) Each location in space and time (pixel) is the calculated relative juvenile growth rate. A value of '0' indicates no growth.

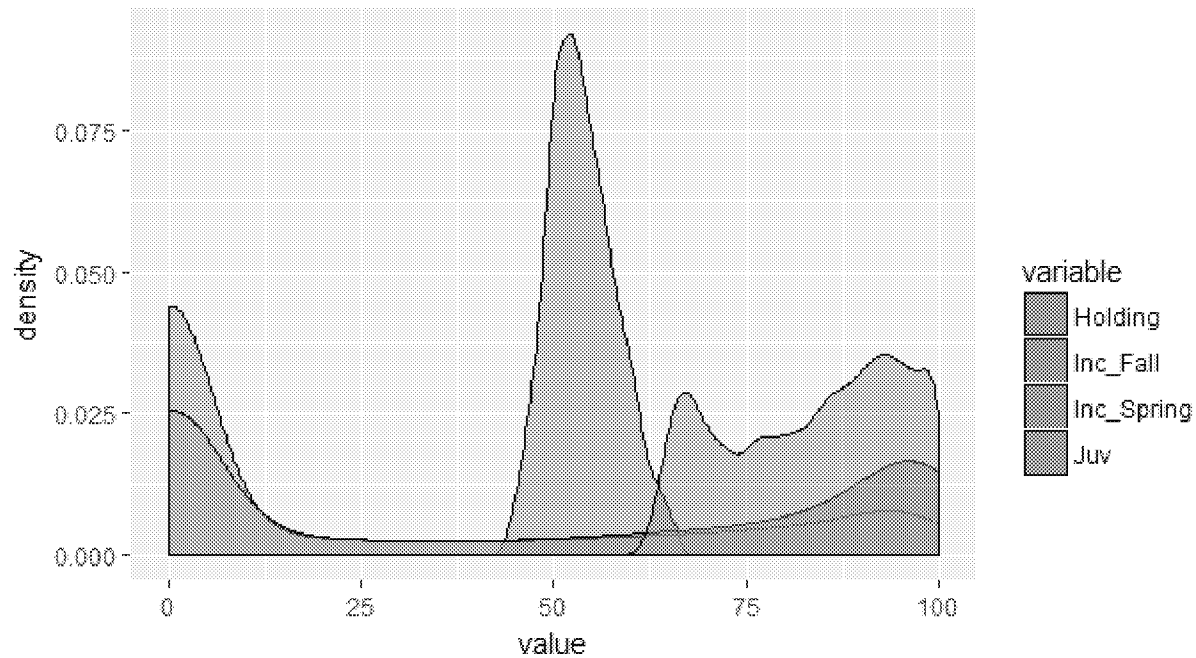


Figure 12. Temperature-dependent effects on multiple life stages along the Yuba River. The X-axis indicates percent effect, and the Y-axis is the total number of observations in space and time. Holding: percent of energy left to allocate to spawning. Incubation: embryo mortality percentage. Juveniles: percent of maximum growth rate. Results are based on when and where salmon occur.

APPENDICES

Appendix 1 Table S1.1. Phenology of life stages of Chinook ESUs and runs in California. Spring-run (green), fall-run (blue), late-fall-run (purple), winter-run (red). CV=Central Valley, LC=Lower Columbia, MC= Mid-Columbia, SONCC=Southern Oregon & Northern California Coast, UKTR=Upper Klamath Trinity Rivers, UC=Upper Columbia, UWR=Upper Willamette River. Note that CA Coastal spring-run is extinct, and SONCC Spring is mostly extinct. A '0' may indicate a negative or a lack of available information. References are listed in Appendix 1 Table S2.

ESU	Run	Lifestage	Jan	Feb	Mar	Apr	May	Jun	Jul	Aug	Sep	Oct	Nov	Dec	Peak_Median	References
CA Coast Fall	Fall	Mig Adult	1	0	0	0	0	0	0	0	1	1	1	1	11	3,10,12,13,14,17
CA Coast Fall	Fall	Holding Adult	0	0	0	0	0	0	0	0	0	0	0	0	NA	3,10,12,13,14,17
CA Coast Fall	Fall	Spawning	1	0	0	0	0	0	0	0	1	1	1	1	11	3,10,12,13,14,17
CA Coast Fall	Fall	Incubation	1	1	1	1	1	0	0	0	1	1	1	1	1	3,10,12,13,14,17
CA Coast Fall	Fall	Emergence	1	1	1	1	1	0	0	0	0	0	0	1	2.5	3,10,12,13,14,17
CA Coast Fall	Fall	Juv Rearing	0	1	1	1	1	1	1	0	0	0	0	0	4.5	3,10,12,13,14,17
CA Coast Fall	Fall	Outmig Juv	0	1	1	1	1	1	1	0	0	0	0	0	4.5	3,10,12,13,14,17
CA Coast Fall	Fall	Ocean Entry	0	0	0	1	1	1	0	0	0	0	0	0	5	3,10,12,13,14,17
CA Coast Spring	Spring	Mig Adult	0	0	1	1	1	1	1	1	0	0	0	0	5.5	3,10,12,13,14,17
CA Coast Spring	Spring	Holding Adult	0	0	1	1	1	1	1	1	0	0	0	0	5.5	3,10,12,13,14,17
CA Coast Spring	Spring	Spawning	0	0	0	0	0	0	0	0	1	1	1	1	10.5	3,10,12,13,14,17
CA Coast Spring	Spring	Incubation	1	1	0	0	0	0	0	0	1	1	1	1	11.5	3,10,12,13,14,17
CA Coast Spring	Spring	Emergence	1	1	0	0	0	0	0	0	0	0	0	1	1	3,10,12,13,14,17
CA Coast Spring	Spring	Juv Rearing	1	1	1	1	1	1	1	1	1	1	0	1	5	3,10,12,13,14,17
CA Coast Spring	Spring	Outmig Juv	0	0	0	0	1	1	1	1	1	1	0	0	7.5	3,10,12,13,14,17
CA Coast Spring	Spring	Ocean Entry	0	0	0	0	1	1	1	1	1	1	0	0	7.5	3,10,12,13,14,17
CA CV Fall	Fall	Mig Adult	1	0	0	0	0	1	1	1	1	1	1	1	10	3,10,12,13,17,26
CA CV Fall	Fall	Holding Adult	0	0	0	0	0	0	0	0	0	0	0	0	NA	3,10,12,13,17
CA CV Fall	Fall	Spawning	1	0	0	0	0	0	0	0	1	1	1	1	10.5	3,10,12,13,17,26
CA CV Fall	Fall	Incubation	1	1	1	1	1	0	0	0	1	1	1	1	1	3,10,12,13,17, 19
CA CV Fall	Fall	Emergence	1	1	1	1	1	0	0	0	0	0	0	1	2.5	3,10,12,13,17, 19
CA CV Fall	Fall	Juv Rearing	1	1	1	1	1	1	0	0	0	0	0	1	3	3,10,12,13,17
CA CV Fall	Fall	Outmig Juv	1	1	1	1	1	1	1	0	0	0	0	0	3.5	3,10,12,13,17,28
CA CV Fall	Fall	Ocean Entry	0	0	1	1	1	1	1	0	0	0	0	0	5	3,10,12,13,17
CA CV Late-Fall	Late-Fall	Mig Adult	1	1	1	1	0	0	0	0	0	1	1	1	12	3,10,12,13,17,19,26
CA CV Late-Fall	Late-Fall	Holding Adult	0	0	0	0	0	0	0	0	0	0	0	0	NA	3,10,12,13,17
CA CV Late-Fall	Late-Fall	Spawning	1	1	1	1	0	0	0	0	0	0	0	1	2.5	3,10,12,13,17,26